Mechanics & Industry **22**, 47 (2021)
© P. Tkach et al., Published by EDP Sciences 2021
https://doi.org/10.1051/meca/2021044

Mechanics & Industry

Available online at:
www.mechanics-industry.org

REGULAR ARTICLE

OPEN ACCESS

High load capacity spur gears with conchoidal path of contact

Pavlo Tkach[1], Pavlo Nosko[2], Oleksandr Bashta[2], Yurii Tsybrii[3,*], and Oleksii Nosko[3]

[1] E.O. Paton Electric Welding Institute of the National Academy of Sciences of Ukraine, 11 K. Malevycha st., Kyiv 03150, Ukraine
[2] National Aviation University, Department of Engineering Science, 1 L. Huzara ave., Kyiv 03058, Ukraine
[3] Bialystok University of Technology, Faculty of Mechanical Engineering, 45C Wiejska st., Bialystok 15351, Poland

Received: 22 September 2020 / Accepted: 13 October 2021

Abstract. The present study is devoted to investigation of spur gears with a conchoidal path of contact and a convex-convex contact between teeth. The load capacity and energy efficiency were evaluated using both theoretical and experimental approaches. The theoretical analysis showed that the conchoidal gear pairs are 5–21% stronger in terms of contact stress and have similar energy efficiency as compared to the involute gear pairs of the same configuration. Experiments were conducted on a gear test rig. Its energy efficiency was determined by measuring the active power of the motor driving the pinion shaft and controlling the torque at the gear shaft. The load capacity of the tested gear pair was estimated by analysing changes in the energy efficiency. It was found that the conchoidal gear pair has more than 20% higher load capacity and slightly higher energy efficiency, which agrees well with the mentioned theoretical results. Thereby, the study concludes a substantially higher load capacity of the conchoidal gears compared to the traditional involute ones.

Keywords: Spur gears / involute gears / conchoidal path of contact / load capacity / contact strength / energy efficiency

1 Introduction

Gears are widely used to transmit motion and energy in mechanical systems. It is difficult to imagine a modern transport machine that does not include gear trains. The most commonly used gears have teeth with an involute active profile generated by straight lines. The set of instantaneous contact points between such teeth forms a straight path of contact. The advantages of involute gears include high manufacturability, relatively small sensitivity to centre distance errors and simplicity of the reference profile. However, relatively large curvatures of the mating teeth result in large contact stresses, which strongly limits the load capacity of involute gears. Therefore, development of non-involute gear drives has a significant scientific and practical interest.

Helical gears with a circular-arc tooth profile were proposed by Wildhaber [1] and Novikov [2], subsequently called 'Wildhaber-Novikov gears'. Novikov's idea is that the contact between gears should take place at a point moving along a tooth. The active profile of one tooth is generated by a convex arc, while that of the mating tooth is generated by a concave arc of a slightly larger radius. Accordingly, the convex-concave contact between teeth is characterised by a reduced curvature, which leads to smaller contact stresses. But a serious disadvantage of Wildhaber-Novikov gears can be found in increased bending stresses in teeth due to the point contact. A comprehensive analysis of this type of gears was performed in the studies [3,4].

Wildhaber-Novikov concept of gearing served as the basis for the development of various circular-arc tooth profiles. One of the successful technical solutions is the application of double circular-arc tooth profile helical gears [5] (p. 158). The reference profile for generating teeth active profiles is composed of two conjugated circular arcs: convex addendum arc and concave dedendum arc. Accordingly, the convex addendums interact with the concave dedendums of the respective pinion and gear teeth. The parameters of two circular arcs are sought to minimise both contact stresses and bending stresses in teeth [6]. The other known technical solutions include (but are not limited to) gears with basic rack of combined circular and involute profile [7], circular-arc tooth pinion on involute tooth gear [8], point-line meshing gears [9], circular-arc curvilinear tooth gears [10], stepped triple circular-arc tooth gears [11], double circular-arc tooth gears modified by tooth end relief with helix [12], double circular-arc tooth gears optimised for harmonic drives [13].

* e-mail: y.tsybrii@pb.edu.pl

This is an Open Access article distributed under the terms of the Creative Commons Attribution License (https://creativecommons.org/licenses/by/4.0), which permits unrestricted use, distribution, and reproduction in any medium, provided the original work is properly cited.

As concerns spur gears, various alternative tooth shapes were proposed to improve the load capacity of gear drives. It is important to name, for instance, gears with zero relative curvature at many contact points [14], gears with linear profile modification [15], gears with quadratic parametric tooth profile [16], tooth profile relief design gears [17], asymmetric tooth gears [18], gears designed by usage of NURB deviation function technique [19], gears designed by B-spline curve fitting and sweep surface modelling [20], gears with multi-segment path of contact [21], cosine tooth gears [22], s-gears designed for wind power turbine operating conditions [23], gears with parabolic path of contact [24], gears with a constant relative curvature [25], gears with a circular arc contact path [26]. Although the mentioned technical solutions were shown to be effective for particular applications and operating conditions, their widespread implementation is limited by the difficulties related to manufacturing complex-shaped teeth.

A relatively simple double circular-arc reference profile for spur gears was proposed in the study [27]. The path of contact of these gears represents a conchoid of Nicomedes. Therefore, they are sometimes referred to as 'conchoidal path-of-contact gears' or 'conchoidal gears'. The study [28] investigated the conchoidal gears with convex-concave contact between teeth and concluded their better meshing and performance characteristics compared to the involute gears. Their disadvantage, however, is an increased sensitivity to manufacturing and mounting errors [29] (p. 33). The study [30] showed that the tooth profiles of the conchoidal gears can be designed to allow a convex-convex contact, which can potentially eliminate the mentioned above disadvantage. To the best authors' knowledge, this potentially promising type of conchoidal gears has not been investigated in terms of load capacity and energy efficiency yet. With this in mind, the purpose of the present study was to theoretically and experimentally investigate the load capacity of the conchoidal path-of-contact spur gears with convex-convex contact between teeth as compared to the traditional involute gears.

2 Theory

2.1 Geometry of the conchoidal gears

Figure 1 presents a geometric description of the conchoidal gears under consideration. Figure 1a shows the generating surface defined in a coordinate system $x_g O_g y_g$. Figure 1b introduces the pitch circles of the pinion 1 and gear 2 and the path of contact. Note that the coordinate systems $x_1 O_1 y_1$ and $x_2 O_2 y_2$ are aligned with the respective pinion 1 and gear 2, whereas XOY is the fixed coordinate system with centre O at the pitch point.

The generating surface is based on the reference profile shown in Figure 1c. The curves O_gA and O_gB form the active profile of a tooth, while O'_gA' and O'_gB' form the active profile of the adjacent tooth. The curve AA' is responsible for generation of the tooth root fillet.

The coordinates of the tooth active profile are expressed separately for the curve O_gA

$$\begin{aligned} x_g &= x - a + \rho \sin\alpha; \\ y_g &= b - \rho \cos\alpha \end{aligned} \tag{1}$$

curve O_gB

$$\begin{aligned} x_g &= x + a - \rho \sin\alpha; \\ y_g &= -b + \rho \cos\alpha \end{aligned} \tag{2}$$

curve O'_gA'

$$\begin{aligned} x_g &= x - a + \rho \sin\alpha; \\ y_g &= \pi/2 - b + \rho \cos\alpha \end{aligned} \tag{3}$$

and curve O'_gB'

$$\begin{aligned} x_g &= x + a - \rho \sin\alpha; \\ y_g &= \pi/2 + b - \rho \cos\alpha. \end{aligned} \tag{4}$$

Here α is the reference profile angle varying from α_w to α_{max}; α_w is the reference profile angle at the pitch line (point O_g); α_{max} is the maximum reference profile angle (points A and B); ρ is the profile circle radius; x is the reference profile shift coefficient; parameters a and b are given by

$$\begin{aligned} a &= \rho \sin\alpha_w; \\ b &= \rho \cos\alpha_w. \end{aligned}$$

It is important to note that equations (1)–(4) and the following equations incorporating geometric parameters are normalised for the module m equal to 1 mm.

Assume that the reference profile is symmetrical. Then it is sufficient to consider the active profile formed only by the curves O_gA and O_gB. The coordinates of the active profile, given by equations (1) and (2), are represented in a concise form:

$$\begin{aligned} x_g &= a \mp a \pm \rho \sin\alpha; \\ y_g &= \pm b \mp \rho \cos\alpha \end{aligned} \tag{5}$$

where the upper and lower signs stand for the curves O_gA and O_gB, respectively.

In the meshing of the generating surface and a tooth being generated, the vector of the relative velocity must be perpendicular to the line normal to the generating surface at the contact point [6]. As applied to the conchoidal gears, this condition allows writing the equation of meshing as

$$\pm b \mp \rho \cos\alpha + (x \mp a \pm \rho \sin\alpha) \cot\alpha - \varphi_{1,2} r_{w1,2} = 0 \tag{6}$$

which represents the relationship between α and the angle $\varphi_{1,2}$ of rotation of the pinion/gear. Here $r_{w1,2}$ is the pitch

MOST WIEDZY Downloaded from mostwiedzy.pl

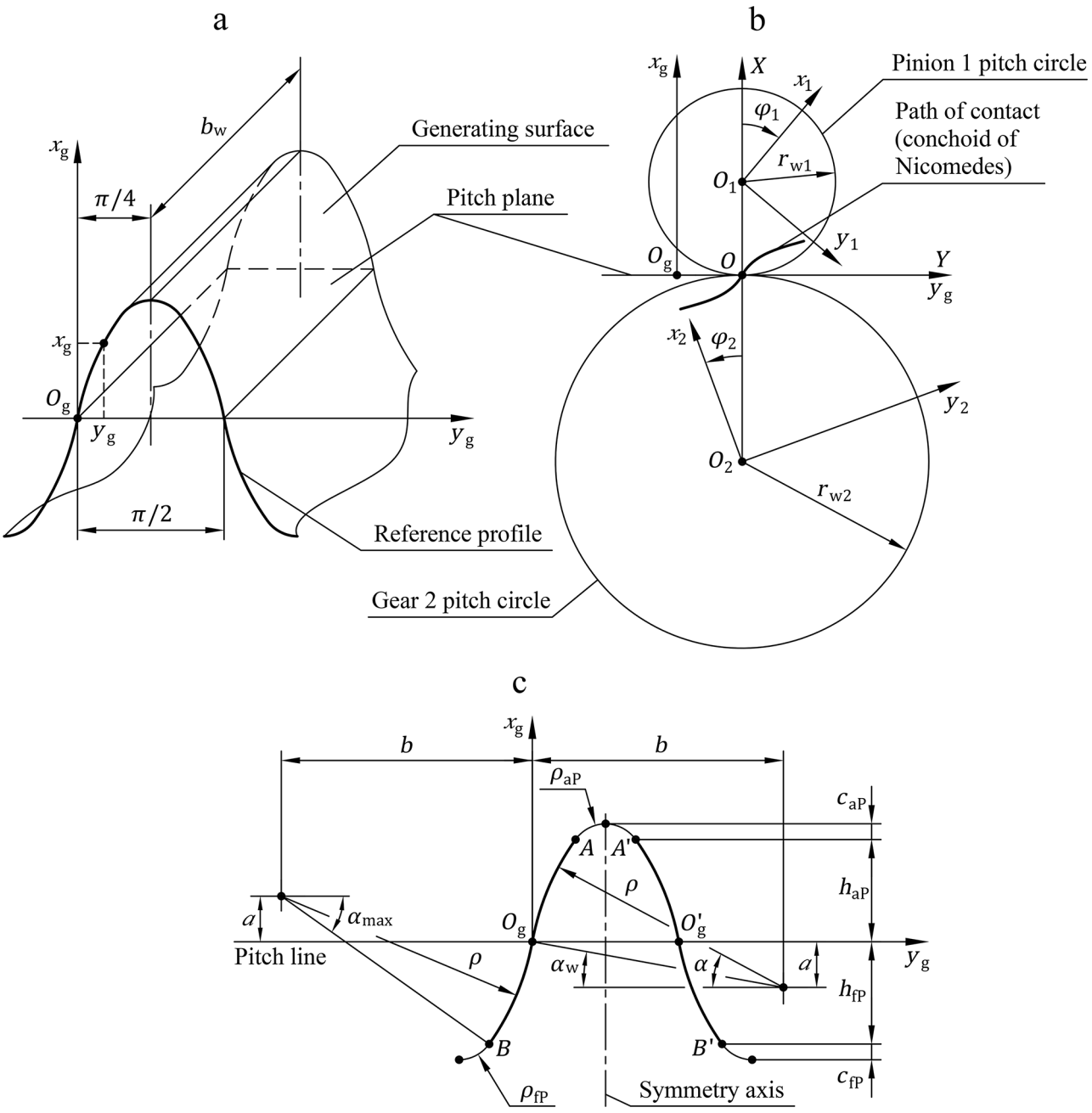

Fig. 1. Geometry of conchoidal gears: (a) generating surface; (b) pinion 1 and gear 2; (c) reference profile.

circle radius of the pinion/gear. As the pitch circles mesh without sliding, it is true that $\varphi_1 r_{w1} = \varphi_2 r_{w2}$.

The equation of the path of contact can be formulated in the coordinate system XOY based on equations (5) and (6) in the form

$$\begin{aligned} X &= x \mp a + \rho\cos(\alpha + \pi \pm \pi/2); \\ Y &= (x \mp a)\tan(\alpha + \pi \pm \pi/2) \\ &\quad + \rho\sin(\alpha + \pi \pm \pi/2) \end{aligned}$$

which coincides with the expression for the conchoid of Nicomedes with angle $(\alpha + \pi \pm \pi/2)$ and parameters $(x \mp a)$ and ρ.

From equation (6) one can also derive the equations for the pinion active profiles

$$\begin{aligned} x_1 &= (x \mp a \pm \rho\sin\alpha + r_{w1})\cos\varphi_1 \\ &\quad + (x \mp a \pm \rho\sin\alpha)\cos\alpha\sin\varphi_1; \\ y_1 &= (x \mp a \pm \rho\sin\alpha + r_{w1})\sin\varphi_1 \\ &\quad - (x \mp a \pm \rho\sin\alpha)\cot\alpha\cos\varphi_1 \end{aligned} \tag{7}$$

MOST WIEDZY Downloaded from mostwiedzy.pl

Table 1. Parameters of the simulated reference profiles normalised for $m = 1$ mm.

Code name	α20	α25	α28
Reference profile angle α_w at pitch line,°	19.6	24.85	27.97
Maximum reference profile angle α_{max},°	23	28	30.69
Distance a	6.072	8.545	10.18
Distance b	17.05	18.448	19.176
Profile circle radius ρ	18.101	20.33	21.71
Tooth addendum height h_{ap}	1	1	0.9
Tooth dedendum height h_{fP}	1	1	0.9
Tooth tip fillet radius ρ_{aP}	0.4297	0.3266	0.3247
Tooth root fillet radius ρ_{fP}	0.4297	0.3266	0.3247
Tooth tip clearance c_{aP}	0.2618	0.1733	0.1589
Tooth root clearance c_{fP}	0.2618	0.1733	0.1589

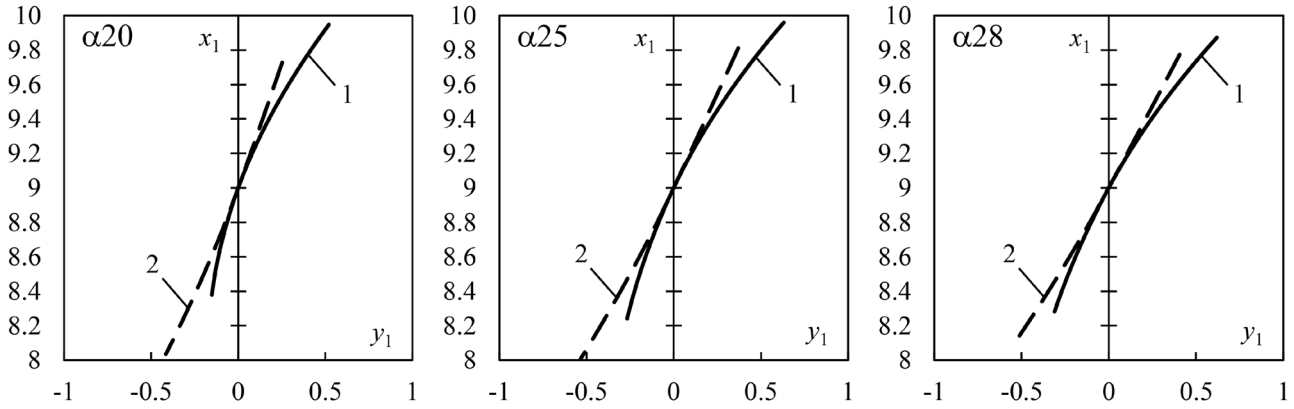

Fig. 2. Geometry of the teeth active profiles of the pinion 1 and gear 2.

and gear active profiles

$$\begin{aligned} x_2 &= (x \mp a \pm \rho \sin\alpha - r_{w2}) \cos\varphi_2 \\ &\quad -(x \mp a \pm \rho \sin\alpha) \cot\alpha \sin\varphi_2; \\ y_2 &= (x \mp a \pm \rho \sin\alpha - r_{w2}) \sin\varphi_2 \\ &\quad -(x \mp a \pm \rho \sin\alpha) \cot\alpha \cos\varphi_2 \end{aligned} \tag{8}$$

in the respective coordinate systems $x_1O_1y_1$ and $x_2O_2y_2$.

Equations (6)–(8) allow thus finding the coordinates of the contact point and the points of the active profiles for specified values of φ_1 and φ_2.

Depending on the geometric parameters, the contact between teeth in a conchoidal gear pair can be of convex-concave or convex-convex type. The present study focusses on investigation of the convex-convex contact which takes place under the condition [30] that

$$a - x \geq r_{w2} \sin^2 \alpha_{max}.$$

The following analysis requires specification of the parameters of the simulated reference profiles and gear pairs. The angle α_w of 20° is the most common, while it can be 25° or even 28° in special gear transmissions [31] (p. 75, 143). Table 1 describes three reference profiles, code-named as 'α20', 'α25' and 'α28', with α_w close to the mentioned values.

Figure 2 shows the teeth profiles of the pinion 1 and gear 2 generated by the reference profiles of Table 1. The profiles of the pinion 1 are determined due to equation (7) in the coordinate system $x_1O_1y_1$ (solid lines), while the profiles of the gear 2 are determined due to equation (8) in the coordinate system $x_2O_2y_2$ (dashed lines). In both cases, the values of $\varphi_{1,2}$ are calculated by equation (6). For the sake of clarity, the profiles of the gear 2 are shown not in its own coordinate system but are meshed with the respective profiles of the pinion at $\varphi_1 = 0$. The geometry of the teeth corresponds to $u = z_2/z_1 = 72/18$ and is normalised for $m = 1$ mm.

The shift of the reference profile has a significant influence on the performance of the gear pair. Table 2 presents three simulated cases: zero shift ('x0'), 0.3 shift ('x0.3') and 0.5 shift ('x0.5').

Finally, Table 3 presents the parameters of the simulated gear pairs and operating conditions. Two gear pairs, code-named as 'u2.4' and 'u4', have the same parameters except for the number z_1 of the pinion teeth and, accordingly, gear ratio $u = z_2/z_1$.

MOST WIEDZY Downloaded from mostwiedzy.pl

Table 2. Shift coefficient x of the simulated reference profile normalised for $m = 1$ mm.

Code name	x0	x0.3	x0.5
Pinion shift	0	+0.3	+0.5
Gear shift	0	−0.3	−0.5

Table 3. Parameters of the simulated gear pairs and operating conditions.

Code name	u2.4	u4
Gear ratio u	2.4	4
Number z_1 of pinion teeth	30	18
Number z_2 of gear teeth	72	
Module m, mm	10	
Effective face width b_w, mm	100	
Elastic modulus E, GPa	210	
Brinell hardness number BHN	250	
Active profile roughness R_a, μm	3.2	
Oil kinematic viscosity ν, mm^2/s	20	
Pinion angular velocity ω_1, rad/s	100	
Pinion torque T_1, Nm	2000	

2.2 Contact strength

The instantaneous mechanical contact of two gear teeth is often treated as the contact between two cylinders with parallel axes. The relationship between the stress σ_H and normal force F_n in the contact zone is then defined by the Hertz equation. If the pinion and gear are made of the same steel with elastic modulus E, this equation takes the form [5]

$$\sigma_H = 0.418\sqrt{\frac{F_n E}{b_w R_r}} \tag{9}$$

where R_r is the reduced curvature radius of the active profiles of the mating teeth at the contact point; b_w is the effective face width.

For the conchoidal gear pair, it yields from equations (5)–(8) that

See equation below.

$$R_{r\ con} = \frac{\left(r_{w1}\frac{\sin^3\alpha}{\sin\alpha_w} + x \mp a \pm \rho\sin\alpha\right)\left(r_{w2}\frac{\sin^3\alpha}{\sin\alpha_w} - x \pm a \mp \rho\sin\alpha\right)}{(r_{w1}+r_{w2})\sin\alpha_w}.$$

$$\theta_{con}^2 = R_{r\ con}\cos\alpha = \frac{\left(r_{w1}\frac{\sin^3\alpha}{\sin\alpha_w} + x \mp a \pm \rho\sin\alpha\right)\left(r_{w2}\frac{\sin^3\alpha}{\sin\alpha_w} - x \pm a \mp \rho\sin\alpha\right)\cos\alpha}{(r_{w1}+r_{w2})\sin\alpha_w} \tag{12}$$

On the other hand, following the study [28], one can derive a similar expression for the involute gear pair:

$$R_{r\ inv} = \frac{(r_{w1}\sin^2\alpha_w + x + x_g)(r_{w2}\sin^2\alpha_w - x - x_g)}{(r_{w1}+r_{w2})\sin^3\alpha_w}.$$

The normal force F_n in the contact zone is expressed via the pinion torque T_1 as

$$F_n = \frac{kT_1}{r_{w1}\cos\alpha} \tag{10}$$

where $k = 1$ for one-pair contact and $k = 0.5$ for double-tooth contact.

Substitution of equation (10) into equation (9) leads to the equation

$$\sigma_H = \frac{0.418}{\theta}\sqrt{\frac{kT_1 E}{b_w r_{w1}}} \tag{11}$$

where the coefficient θ given by

$$\theta = \sqrt{R_r\cos\alpha}$$

depends solely on the geometry of the active profiles. According to equation (11), θ is inverse proportional to σ_H and, thereby, can serve as the measure of contact strength.

Based on the expressions of $R_{r\ con}$ and $R_{r\ inv}$ above, one easily finds θ for the conchoidal gear pair:

See equation (12) below.

and for the involute gear pair:

$$\theta_{inv}^2 = R_{r\ inv}\cos\alpha_w = \frac{(r_{w1}\sin^2\alpha_w + x + x_g)(r_{w2}\sin^2\alpha_w - x - x_g)\cos\alpha_w}{(r_{w1}+r_{w2})\sin^3\alpha_w}. \tag{13}$$

Note that θ_{con} of equation (12) is a function of α, while θ_{inv} of equation (13) is a function of x_g.

Figure 3 illustrates the variation ranges of the ratio $\theta_{con}/\theta_{inv}$ calculated by equations (12) and (13) for the reference profiles and gear pairs specified in Tables 1–3. The limit values of each variation range correspond to the limit points of the path of contact. It is seen that for all

MOST WIEDZY Downloaded from mostwiedzy.pl

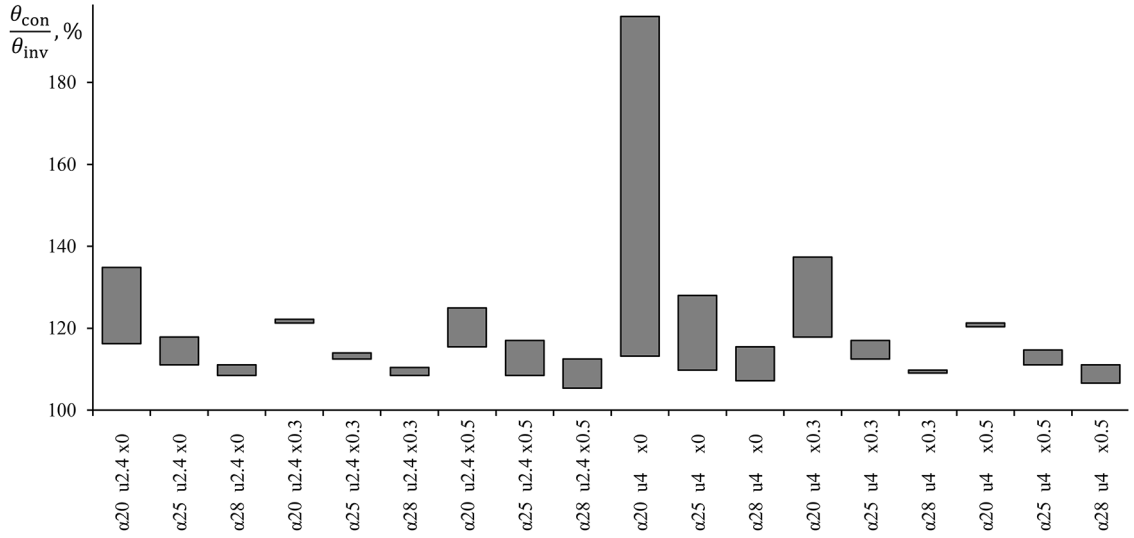

Fig. 3. Ratio between contact strength coefficients θ_{con} and θ_{inv}.

combinations under consideration, $\theta_{con}/\theta_{inv}$ is noticeably larger than 100%. The lower limit of $\theta_{con}/\theta_{inv}$ varies between 105% and 121%, implying that the conchoidal gear pairs have 5–21% higher contact strength compared to the involute gear pairs of the same configuration. An exceptional case is 'α20 u4 x0', implying $\alpha_w = 20°$, $u = 4$ and $x = 0$, at which the upper limit of $\theta_{con}/\theta_{inv}$ is about 200%. This case is characterised by a close to zero curvature radius at the tooth dedendum of the pinion and, therefore, is eliminated from consideration. It is notable that $\theta_{con}/\theta_{inv}$ decreases substantially as α_w increases.

2.3 Energy efficiency

The active profiles of the mating teeth slide relative each other at the contact point with velocity υ_g. This is inevitably accompanied by the friction process which is characterised by friction coefficient μ. Introduce the energy efficiency of a gear pair as follows:

$$\eta = 1 - \frac{z_1}{2\pi T_1 \omega_1} \int_{\varphi_{11}}^{\varphi_{12}} \mu F_n \upsilon_g d\varphi \qquad (14)$$

where ω_1 is the angular velocity of the pinion; φ_{11} and φ_{12} are the angles of the pinion rotation which correspond to the start and end of the meshing phase. The start contact point and end contact point in the meshing of the pinion and gear are defined in the generating process by the points of the reference profile with angle α_{max1} at $\varphi_1 = \varphi_{11}$ and angle α_{max2} at $\varphi_1 = \varphi_{12}$, respectively. The values of α_{max1} and α_{max2} are found by the equations below:

See equation below.

The integral term in equation (14) indicates the fraction of the input power that transforms into friction heat over one meshing phase from φ_{11} to φ_{12}.

For the conchoidal gear pair, the sliding velocity is derived from equations (5) and (6) as

$$\upsilon_{g\ con} = \omega_1 \frac{u+1}{u} \frac{x \pm \rho(\sin\alpha - \sin\alpha_w)}{\sin\alpha}$$

while for the involute gear pair, it can be expressed in our notation as

$$\upsilon_{g\ inv} = \omega_1 \frac{u+1}{u} \frac{x + x_g}{\sin\alpha_w}.$$

For steel-on-steel gear teeth contacts, the friction coefficient μ is well approximated by the empirical function [32,33]

$$\mu = 0.09\left(10 + \lg\left(\frac{\text{BHN } R_a}{ER_r}\right)\right) \frac{(F_n/b_w)^{0.1}}{\nu^{0.07}\upsilon_\Sigma^{0.1}\upsilon_g^{0.35}R_r^{0.25}} \qquad (15)$$

where BHN is the Brinell hardness number; R_a is the roughness parameter; ν is the oil kinematic viscosity; υ_Σ is the sum of the velocity components of the active profiles at the contact point perpendicular to the line of contact [31] (p. 182). The quantities in equation (15) should be specified in the following units of measurements: BHN and E in the same units; F_n in N; b_w in mm; R_r and R_a in cm; ν in mm^2/s; υ_g and υ_Σ in cm/s.

$$(r_{w1} + h_{aP})^2 = (r_{w1} + \rho\sin\alpha_{max1} - a + x)^2 + (\rho\sin\alpha_{max1} - a + x)^2\cot^2\alpha_{max1};$$
$$(r_{w2} + h_{fP})^2 = (r_{w2} + \rho\sin\alpha_{max2} - a - x)^2 + (\rho\sin\alpha_{max2} - a + x)^2\cot^2\alpha_{max2}.$$

MOST WIEDZY Downloaded from mostwiedzy.pl

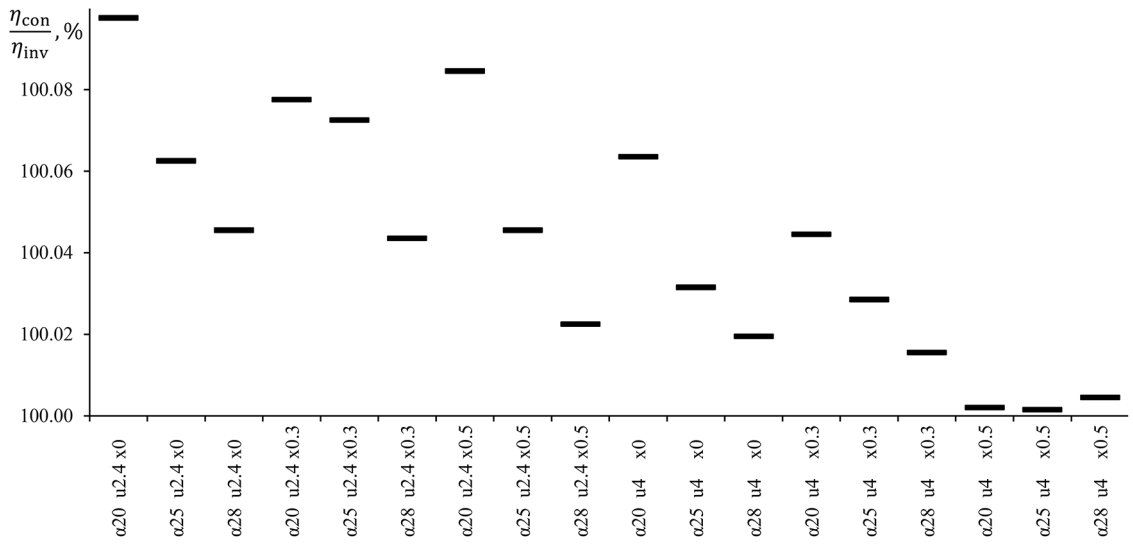

Fig. 4. Ratio between energy efficiencies η_{con} and η_{inv}.

The formula to calculate υ_Σ for the conchoidal gear pair is obtained from equations (5) and (6) in the form

$$\upsilon_{\Sigma\ con} = \omega_1\left(\frac{u-1}{u}\frac{\rho(\sin\alpha - \sin\alpha_w)\pm x}{\sin\alpha} \mp \frac{2r_{w1}\rho\sin^2\alpha}{\rho\sin\alpha_w + x}\right)$$

while for the involute gear pair, it reads

$$\upsilon_{\Sigma\,inv} = \omega_1\left(\frac{u-1}{u}\frac{x_g + x}{\sin\alpha_w} + 2r_{w1}\sin\alpha_w\right).$$

Figure 4 shows the values of the ratio between the energy efficiencies η_{con} and η_{inv} calculated by equation (14) for the respective conchoidal and involute gear pairs. It is seen that η_{con} is up to 0.1% larger than η_{inv} for all considered combinations, suggesting that the conchoidal gear pairs have similar energy efficiency as the involute gear pairs of the same configuration. This result is explained by the fact that μ of equation (15) takes a smaller value in the case of conchoidal gear pair, which is due to the inequalities $\upsilon_{\Sigma\,con} > \upsilon_{\Sigma\,inv}$ and $R_{r\,con} > R_{r\,inv}$.

3 Experimental study

The foregoing theoretical analysis showed that the conchoidal gear pairs have a substantially higher contact strength and similar energy efficiency if compared to the involute gear pairs with the same parameters. These findings should undergo experimental validation to be accepted. This section describes an experimental study of the conchoidal and involute gear pairs in terms of the mentioned characteristics.

3.1 Tooth-cutting tool

A hob cutter was designed and manufactured for cutting conchoidal gear pairs. It was made of P18 steel due to GOST 19265-73 (EN X75WCrV18-4-1) and heat treated to Rockwell hardness HRC 65. The parameters of the hob cutter are presented in Table 4, while its tooth profile is schematically shown in Figure 5. The parameters of the

Table 4. Hob cutter parameters.

Parameter	Value
Module m, mm	1.95
Number of threads	1
Number of teeth	12
Normal pitch, mm	6.126
Axial pitch, mm	6.128
Reference diameter, mm	84.086
Lead angle,°	1.317

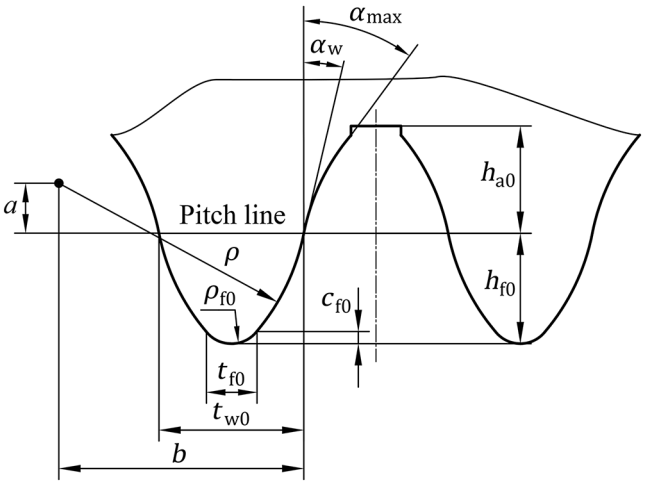

Fig. 5. Hob cutter tooth profile.

MOST WIEDZY Downloaded from mostwiedzy.pl

Table 5. Reference profile parameters.

Parameter	Formula	Value
Module m, mm		1.95
Backlash δ, mm		0.2
Reference profile angle α_w at pitch line,°		19.6
Maximum reference profile angle α_{max},°		23
Distance a, mm	$a = 6.072m$	11.84
Distance b, mm	$b = 17.05m$	33.248
Profile circle radius ρ, mm	$\rho = 18.101m$	35.297
Tooth thickness t_{w0} at pitch line, mm	$t_{w0} = \pi m/2 + \delta$	3.263
Tooth thickness t_{f0} at height (h_{f0}–c_{f0}), mm	$t_{f0} = 0.791m$	1.542
Tooth root fillet ρ_{f0}, mm	$\rho_{f0} = \frac{t_{f0} + \delta}{2\cos\alpha_{max}}$	0.946
Tooth root clearance c_{f0}, mm	$c_{f0} = \rho_{f0}(1 - \sin\alpha_{max})$	0.576
Tooth dedendum height h_{f0}, mm	$h_{f0} = m + c_{f0}$	2.526
Tooth addendum height h_{a0}, mm	$h_{a0} = h_{f0}$	2.526

reference profile were calculated using the formulae given in Table 5.

3.2 Tested gear pairs

Using the hob cutter, 3 conchoidal gear pairs were manufactured. Further 3 involute gear pairs were manufactured using a standard hob cutter of the same module. All gears were cut out of 40X steel (EN 41Cr4) due to GOST 4543-71 364. Table 6 presents its mechanical properties. The conchoidal and involute gear pairs had the same configuration presented in Table 7. Note that they were manufactured with the reference profile shift corresponding to 'x0.5' (see Tab. 2).

The pinion and gear of the tested gear pair (conchoidal or involute) were installed on the shafts supported by bearings inside a gear box. An oil bath lubrication method with natural convection was used. The gears were lubricated by an AK15 motor oil. The level of oil in the gear box was regularly monitored.

3.3 Gear test rig

The tests were carried out using a gear test rig shown in Figure 6. The principal units of the test rig were an electric motor, the gear box with the tested gear pair inside and an electromagnetic powder brake. The motor of rated power 15 kW applied torque T_1 to the pinion shaft and drove it with angular velocity ω_1 of 153.9 rad/s. The brake allowed controlling the torque T_2 at the gear shaft by measuring displacements of an elastic element. The motor, gear box and brake were dead mounted to a massive basement with bolts. The shafts of the mentioned units were connected by flexible couplings. An accurate alignment of the shafts was provided. The measurement system of the test rig allowed measuring the active power $P = T_1\omega_1$ of the motor, the gear torque T_2 and the temperature ϑ of the oil in the gear box.

Table 6. Gear steel mechanical properties.

Property	Value
Elastic modulus E, GPa	210
Brinell hardness number BHN	270
Fatigue contact stress $\sigma_{H\ lim}$, MPa	610
Allowable contact stress $[\sigma_H]$, MPa	483
Base number $N_{H\ lim}$ of cycles	$2 \cdot 10^7$

Table 7. Gear pair parameters.

Parameter	Value
Module m, mm	1.95
Number z_1 of pinion teeth	14
Number z_2 of gear teeth	88
Gear ratio u	6.29
Reference profile shift coefficient x	0.5
Pinion pitch circle radius r_{w1}, mm	13.65
Gear pitch circle radius r_{w2}, mm	85.8
Effective face width b_w, mm	60
Active profile roughness R_a, μm	3.2
Oil kinematic viscosity ν, mm^2/s	15

3.4 Research methodology

Each gear pair was tested according to a multi-step procedure developed in the Central Scientific Research Institute of Machine Building and Metalworking (former Soviet Union) intended for conventional gear transmissions, as described in Table 8.

MOST WIEDZY Downloaded from mostwiedzy.pl

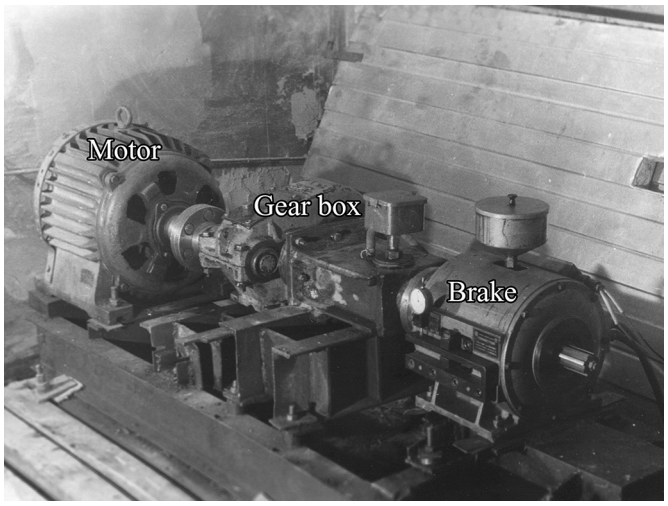

Fig. 6. Gear test rig.

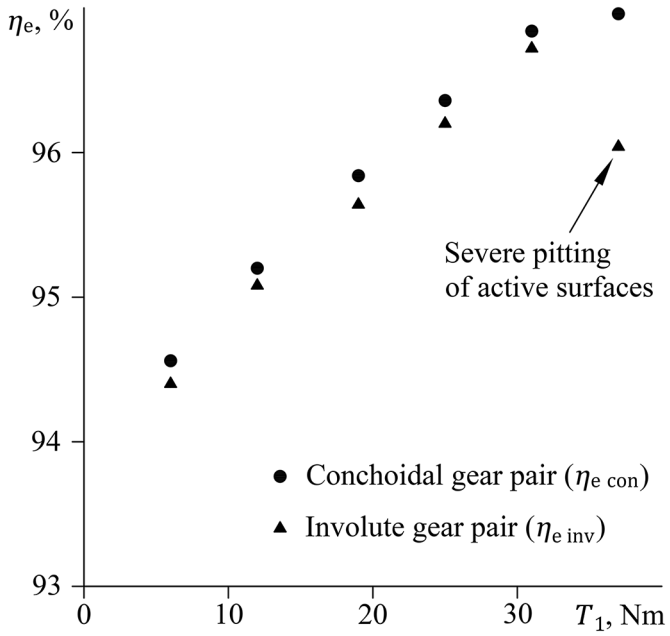

Fig. 7. Gear test rig energy efficiency η_e vs pinion torque T_1.

Table 8. Experimental multi-step procedure.

Loading step	Pinion torque T_1	Total duration
0	idle mode	2 hours
1	$0.2\,[T_1] = 6.2$ Nm	24 hours
2	$0.4\,[T_1] = 12.4$ Nm	24 hours
3	$0.6\,[T_1] = 18.6$ Nm	24 hours
4	$0.8\,[T_1] = 24.8$ Nm	24 hours
5	$1.0\,[T_1] = 31$ Nm	$1.0\,N_{H\ lim} = 2\cdot10^7$ cycles
6	$1.2\,[T_1] = 37.2$ Nm	$1.5\,N_{H\ lim} = 3\cdot10^7$ cycles

Zero step was a 2-hour running-in of the gear pair with the brake off (idle mode). At each next loading step, the gear torque T_2 was increased so that the corresponding pinion torque T_1 increased by $0.2[T_1]$, where $[T_1]$ is the allowable pinion torque. The value of $[T_1]$ was determined based on equation (9) with account of different factors:

$$[T_1] = \frac{1}{K_{H\alpha}K_{H\beta}K_{HV}Z_H^2Z_\varepsilon^2}\frac{b_w r_{w1}^2}{500Z_E^2}\frac{u}{u+1}[\sigma_H]$$

where $[\sigma_H]$ is the allowable contact stress (see Tab. 6); $K_{H\alpha}$ is the factor of non-uniform load distribution between the teeth; $K_{H\beta}$ is the factor of non-uniform load distribution along the contact lines; K_{HV} is the factor of the internal dynamic load in the meshing; Z_E is the factor in view of the mechanical properties of the gears, $\sqrt{\text{MPa}}$; Z_H is the factor in view of the shape of the mating teeth surfaces at the pitch point; Z_ε is the factor in view of the total length of the contact lines. In the equation above, $[T_1]$ is in Nm, $[\sigma_H]$ is in MPa, b_w and r_{w1} are in mm.

At the loading steps 1 to 4, the gear pair was tested for 8 hours per day, with total duration of 24 hours. Accordingly, the state of the active surfaces of the gears was examined after each 8 test hours. After the loading step 4, the used oil was drained from the gear box, the gear box and the components inside it were cleaned, and fresh oil was added. At the loading steps 5 and 6 with respective loads $[T_1]$ and $1.2\,[T_1]$, the gear pair was tested for 8 hours per day, with total number of pinion cycles of $N_{H\ lim}$ and $1.5N_{H\ lim}$, respectively. Here $N_{H\ lim}$ is the base number of cycles (see Tab. 6).

The energy efficiency η_e of the test rig was determined from the known values of the motor active power P, pinion angular velocity ω_1 and gear torque T_2 as follows:

$$\eta_e = \frac{T_2}{T_1 u} = \frac{T_2\omega_1}{Pu}.$$

It is noteworthy that η_e represents the product of the energy efficiencies of all units of the test rig, including the gear box. Since the test rig operated under the same kinematic and loading conditions regardless of gear pair type, one can compare the energy efficiencies of the conchoidal and involute gear pairs based on the ratio between the values of $\eta_{e\,con}$ and $\eta_{e\,inv}$ obtained by testing the respective conchoidal and involute gear pairs.

4 Results and discussion

The experimental data are shown in Figures 7 and 8. Each point indicates the average stationary value obtained from testing 3 gear pairs at a specific loading step.

Figure 7 shows the dependence of the energy efficiencies $\eta_{e\,con}$ and $\eta_{e\,inv}$ on the pinion torque T_1. It is seen that $\eta_{e\,con}$ is systematically 0.1–0.2% larger than $\eta_{e\,inv}$, implying that the conchoidal gear pair is slightly more energy efficient than the involute one. The value of $\eta_{e\,inv}$ at $T_1 = 37.2$ Nm, however, is not in line with the general trend. An after-test

MOST WIEDZY Downloaded from mostwiedzy.pl

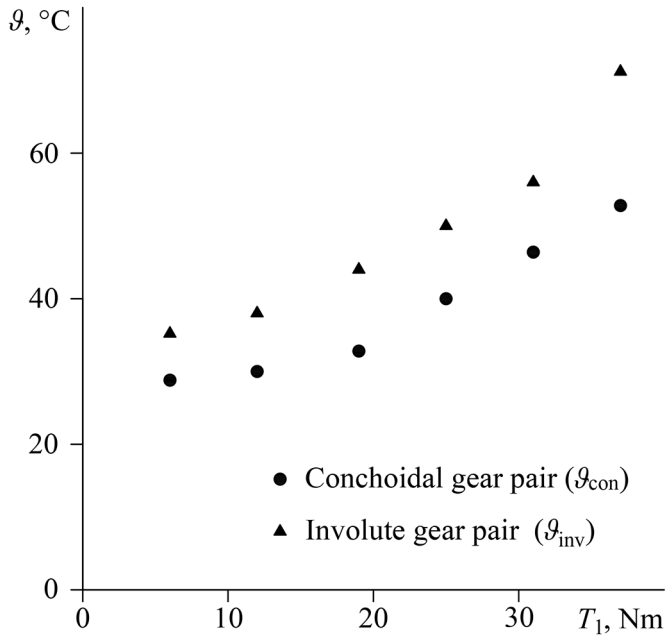

Fig. 8. Gear box oil temperature ϑ vs pinion torque T_1.

visual examination showed that the active surfaces of the involute gears were subjected to severe pitting, whereas the conchoidal gears were damaged insignificantly. This allows to explain the unexpected decrease in $\eta_{e\,inv}$ at $T_1 = 37.2$ Nm.

The data presented in Figure 7 suggest that T_1 of about 31 Nm corresponds to the load capacity of the involute gear pair. On the other hand, the stable growth of $\eta_{e\,con}$ allows stating that the load capacity of the conchoidal gear pair is as minimum as 37.2 Nm, which is 20% larger. This correlates well with the theoretical finding that the conchoidal gear pairs have 5–21% higher contact strength compared to the involute gear pairs of the same configuration.

Figure 8 shows the influences of T_1 on the gear box oil temperatures ϑ_{con} and ϑ_{inv} measured for the respective conchoidal and involute gear pairs. According to the presented values, ϑ_{inv} is substantially larger than ϑ_{con}, i.e., the involute gear pair generates more friction heat than the conchoidal one. This confirms qualitatively the results of Figure 7. It is also seen that the increase in ϑ_{inv} is large at $T_1 = 37.2$ Nm, which is in agreement with the behaviour of $\eta_{e\,inv}$.

For the nominal mode of $T_1 = 31$ Nm, ϑ_{con} is 17% smaller than ϑ_{inv} (see Fig. 8). For the sake of comparison, flash temperatures arising in the contact points of the tested gear pairs operating in the nominal mode were simulated based on Blok's formula [5]. The simulations show that as compared to the involute gear pair, the flash temperature in the conchoidal gear pair is 27% lower for the pinion tooth addendum on gear tooth dedendum contact, 56% lower for the pinion tooth dedendum on gear tooth addendum contact, and on average 20% higher for the teeth contact in the vicinity of the pitch point which is about $0.4m$ in height.

5 Conclusion

The conchoidal path-of-contact spur gears of convex-convex contact type were systematically investigated regarding their load capacity and energy efficiency. The theoretical analysis conducted for different values of the reference profile parameters and gear ratio showed that the conchoidal gear pairs are 5–21% stronger in terms of contact stress and have similar energy efficiency if compared to the traditional involute gear pairs of the same configuration. These findings were experimentally validated using a gear test rig in which the energy efficiency was determined by measuring the active power of the motor driving the pinion shaft for a controlled value of the torque at the gear shaft. The load capacity of the tested gear pair was estimated by analysing the behaviour of the energy efficiency under intensifying loading conditions. It was found that the load capacity of the conchoidal gear pair is higher by more than 20%, while its energy efficiency is slightly higher. A good agreement between the obtained theoretical and experimental results confirms a substantially higher load capacity of the conchoidal gears.

This research did not receive any specific grant from funding agencies in the public, commercial, or not-for-profit sectors.

Notation

a	Geometric parameter
b	Geometric parameter
b_w	Effective face width
c_a	Tooth tip clearance
c_f	Tooth root clearance
h_a	Tooth addendum height
h_f	Tooth dedendum height
m	Module
r_w	Pitch circle radius
u	Gear ratio
v_g	Sliding velocity
x	Reference profile shift coefficient
$x_g O_g y_g$	Coordinate system aligned with reference profile
z	Number of teeth
E	Elastic modulus
F_n	Normal force
$N_{H\ lim}$	Base number of cycles
P	Motor active power
R_a	Roughness parameter
R_r	Reduced curvature radius
T	Torque
$[T_1]$	Allowable pinion torque
XOY	Fixed coordinate system
α	Reference profile angle
α_w	Reference profile angle at pitch line
α_{max}	Maximum reference profile angle
η	Simulated energy efficiency of gear pair
η_e	Measured energy efficiency of gear test rig
θ	Contact strength coefficient
ϑ	Oil temperature
μ	Friction coefficient
ν	Oil kinematic viscosity

MOST WIEDZY Downloaded from mostwiedzy.pl

ρ	Profile circle radius
ρ_a	Tooth tip fillet radius
ρ_f	Tooth root fillet radius
σ_H	Contact stress
$[\sigma_H]$	Allowable contact stress
φ	Angle of rotation
ω_1	Pinion angular velocity
BHN	Brinell hardness number
$_p$	Related to reference profile
$_0$	Related to tooth-cutting tool
$_1$	Related to pinion
$_2$	Related to gear
$_{1,2}$	Related to pinion and gear
$_{con}$	Related to conchoidal gear pair
$_{inv}$	Related to involute gear pair

References

[1] E. Wildhaber, Helical gearing, patent US 1601750, 1926

[2] M.L. Novikov, Gear transmissions and cam mechanisms with a point meshing system, patent SU109113, 1956 (in Russian)

[3] F.L. Litvin, C.B. Tsay, Helical gears with circular arc teeth: simulation of conditions of meshing and bearing contact, J. Mech. Trans. Autom. **107**, 556–564 (1985)

[4] A. Dyson, H.P. Evans, R.W. Snidle, Wildhaber-Novikov circular arc gears: geometry and kinematics, Proc. R. Soc. A **403**, 313–340 (1986)

[5] V.N. Kudrjavcev, J.A. Derzhavec, E.G. Gluharev, Design and calculation of reduction gears, Mashinostroenie, Leningrad, 1971 (in Russian)

[6] F.L. Litvin, J. Lu, Computerized simulation of generation, meshing and contact of double circular-arc helical gears, Math. Comput. Model. **18**, 31–47 (1993)

[7] Y. Ariga, S. Nagata, Load capacity of a new W-N gear with basic rack of combined circular and involute profile, J. Mech. Trans. Autom. **107**, 565–572 (1985)

[8] C.B. Tsay, Z.H. Fong, Computer simulation and stress analysis of helical gears with pinion circular arc teeth and gear involute teeth, Mech. Mach. Theory **26**, 145–154 (1991)

[9] Q. Luo, H. Li, J. Wang, Y. Zhang, H. Huang, Transmission of point-line meshing gear, The Int. J. Adv. Manufactur. Technol. **33**, 845–855 (2007)

[10] Y.C. Wu, K.Y. Chen, C.B. Tsay, Y. Ariga, Contact characteristics of circular-arc curvilinear tooth gear drives, J. Mech. Des. **131**, 181003 (2009)

[11] S.C. Yang, Mathematical model of a stepped triple circular-arc gear, Mech. Mach. Theory **44**, 1019–1031 (2009)

[12] H. Zhang, L. Hua, X. Han, Computerized design and simulation of meshing of modified double circular-arc helical gears by tooth end relief with helix, Mech. Mach. Theory **45**, 46–64 (2010)

[13] X. Chen, Y. Liu, J. Xing, S. Lin, W. Xu, The parametric design of double-circular-arc tooth profile and its influence on the functional backlash of harmonic drive, Mech. Mach. Theory **73**, 1–24 (2014)

[14] T. Komori, Y. Ariga, S. Nagata, A new gears profile having zero relative curvature at many contact points (logiX tooth profile), J. Mech. Des. **112**, 430–436 (1990)

[15] C. Lee, H.H. Lin, F.B. Oswald, D.P. Townsend, Influence of linear profile modification and loading conditions on the dynamic tooth load and stress of high-contact-ratio spur gears, J. Mech. Des. **113**, 473–480 (1991)

[16] M.H. Tsai, Y.C. Tsai, Design of high-contact-ratio spur gears using quadratic parametric tooth profiles, Mech. Mach. Theory **33**, 551–564 (1998)

[17] N. Yildirim, R.G. Munro, A systematic approach to profile relief design of low and high contact ratio spur gears, Proc. Inst. Mech. Eng. C **213**, 551–562 (1999)

[18] A. Kapelevich, Geometry and design of involute spur gears with asymmetric teeth, Mech. Mach. Theory **35**, 117–130 (2000)

[19] T. Yeh, D.C.H. Yang, S.H. Tong, Design of new tooth profiles for high-load capacity gears, Mech. Mach. Theory **36**, 1105–1120 (2001)

[20] S. Barone, Gear geometric design by B-spline curve fitting and sweep surface modelling, Eng. Comput. **17**, 66–74 (2001)

[21] Z.H. Fong, T.W. Chiang, C.W. Tsay, Mathematical model for parametric tooth profile of spur gear using line of action, Math. Comput. Model. **36**, 603–614 (2002)

[22] S. Luo, Y. Wu, J. Wang, The generation principle and mathematical models of a novel cosine gear drive, Mech. Mach. Theory **43**, 1543–1556 (2008)

[23] G. Hlebanja, S-gears for wind power turbine operation conditions, Mach. Des. **4**, 123–130 (2012)

[24] J. Wang, L. Hou, S. Luo, R.Y. Wu, Active design of tooth profiles using parabolic curve as the line of action, Mech. Mach. Theory **67**, 47–63 (2013)

[25] L. Liu, F. Meng, J. Ni, A novel non-involute gear designed based on control of relative curvature, Mech. Mach. Theory **140**, 144–158 (2019)

[26] Y. Wang, S. Ren, Y. Li, Design and manufacturing of a novel high contact ratio internal gear with a circular arc contact path, Int. J. Mech. Sci. **153–154**, 143–153 (2019)

[27] I.R. Shabanov, On the gear transmission with a conchoidal path of contact, Nadyozhnost i Kachestvo Zubchatych Peredach **18-67-106**, 1–8 (1967) (in Russian)

[28] V.P. Shishov, P.L. Nosko, O.A. Revyakina, Cylindrical transmissions with arch teeth, Publishing House of Volodymyr Dahl East Ukrainian National University, Lugansk, 2004 (in Russian)

[29] H.J. Watson, Modern Gear Production, Pergamon Press, Oxford (1970)

[30] V.P. Shishov, O.A. Revyakina, P.N. Tkach, On the character of teeth contact in cylindrical transmissions, Bull. Natl. Tech. Univ. **21**, 110–119 (2007) (in Russian)

[31] H. Linke, J. Börner, R. Heß, Cylindrical Gears: Calculation, Materials, Manufacturing, Carl Hanser Verlag, Munich (2016)

[32] Y.N. Drozdov, V.I. Smirnov, Study of the coefficient of sliding friction for high contact parameters, Vestnik Mashinostroeniya **6**, 19–23 (1977) (in Russian)

[33] V. Onishchenko, Tooth wear modeling and prognostication parameters of engagement of spur gear power transmissions, Mech. Mach. Theory **43**, 1639–1664 (2008)

Cite this article as: P. Tkach, P. Nosko, O. Bashta, Y. Tsybrii, O. Nosko, High load capacity spur gears with conchoidal path of contact, Mechanics & Industry **22**, 47 (2021)

MOST WIEDZY Downloaded from mostwiedzy.pl